CEAS EuroGNC 2019
"Conference on Guidance, Navigation and Control"
3-5 April 2019 @ Politecnico di Milano, Milan, Italy.

CEAS-GNC-2019-066

Cascaded Incremental Backstepping Controller for the Attitude Tracking of Fixed-Wing Aircraft

Rafael A. Cordeiro, José R. Azinheira and Alexandra Moutinho

Abstract Control strategies using Incremental Dynamics (ID) are getting the attention of the aerospace researchers given its robustness and low dependence on accurate aerodynamics model. Previous works proposed cascaded attitude controllers using backstepping strategy and applying ID to design the rate control in the cascaded structure. For a better tracking of the sideslip angle, which is not a truly kinematic variable, we propose the use of the incremental backstepping strategy in both control levels – attitude and rate. The airspeed is included in the rate controller for cruise control. The strategy is applied in simulation to control the attitude of a Boeing 747 aircraft. The results are compared with the previous approach and the performance is evaluated according to the military standard MIL-DTL-9490E.

1 Introduction

Three main motivations guide the development of new technologies in the aeronautics industry: 1) the increase of flight safety; 2) the reduction of development and operation costs; and 3) the increase of the flight performance and the maneuverability of the aircraft. In this scenario, Automatic Flight Control Systems (AFCS) deserve special attention since they can evolve all three desired aspects.

Rafael de Angelis Cordeiro
LAETA/IDMEC – Instituto Superior Técnico, Av. Rovisco Pais 1049-001 Lisboa, Portugal,
e-mail: rafael.a.cordeiro@tecnico.ulisboa.pt

José Raul Azinheira
LAETA/IDMEC – Instituto Superior Técnico, Av. Rovisco Pais 1049-001 Lisboa, Portugal,
e-mail: jose.raul.azinheira@tecnico.ulisboa.pt

Alexandra Moutinho
LAETA/IDMEC – Instituto Superior Técnico, Av. Rovisco Pais 1049-001 Lisboa, Portugal,
e-mail: alexandra.moutinho@tecnico.ulisboa.pt

Nowadays, most commercial AFCS are still based on classical linear control techniques [1], with gain scheduling approaches being used to deal with changes in flight conditions. However, cases like highly dynamic maneuvers or severe structural/actuator failures may lead to an inaccurate control [2]. Additionally, gain scheduling techniques are time-consuming since each flight condition requires the design of several control gains.

In the beginning of the 21st century, AFCS started to be implemented using nonlinear control techniques [3] aiming to increase flight safety and to reduce development time since no scheduling is required. Nonlinear Dynamics Inversion (NDI) and Backstepping (BKS) are two of the nonlinear techniques used in AFCS.

The NDI and BKS techniques are used in many AFCS implementations [4–7], being the F-35 Lightning II the first aircraft to be produced using NDI in its AFCS [8]. However, both nonlinear solutions require highly accurate models of the system to be controlled, that is a costly and time consuming task in which extensive experimentation is necessary to identify the model parameters. A possible alternative is to introduce robust techniques in the NDI or BKS controllers, but these techniques are often very conservative, reducing the flight performance.

The advances in onboard computation hardware and in sensing technologies allow the improvement of the performance of nonlinear controllers. Online identification strategies have been used to develop adaptive nonlinear AFCS and overcome the model uncertainties, but its implementation must be fast enough to guarantee the stability of the adaptive closed-loop system [7].

Another alternative to deal with the model uncertainties is the so-called sensor-based control strategy, in which the precise knowledge of the system is traded by the precise sensing of its dynamics, reducing even more the identification efforts during control synthesis.

A promising sensor-based technique consists on the use of Incremental Dynamics (ID) to obtain controllers less dependent of the system model [9, 10]. This technique produced two new control strategies: the Incremental Nonlinear Dynamics Inversion (INDI) and the Incremental Backstepping (IBKS) [11, 12]. Both INDI and IBKS compute incremental commands employing acceleration feedback (sensor measurements) to extract unmodeled dynamics information. In this way, the design of these sensor-based nonlinear controllers no longer needs the time consuming and costly dynamics-related model data that depends exclusively on the states of the system.

The first concepts of the INDI appeared in [9], named as simplified NDI. Later, the technique was formally developed in [11], becoming known as Incremental NDI. A discussion on the stability limitations of the INDI strategy is presented in [13]. The INDI control strategy has been applied for different aerial vehicles [14–17], highlighting the work of [18], which is the first literature on the experimental application of INDI in a certified passenger aircraft.

As a sequence of INDI research, Acquatella [12] used the incremental dynamics principle in a backstepping approach. IBKS has been studied at an academic level with feasibility studies regarding its potential application to different types of platforms [1, 12, 19, 20].

In the literature, INDI and IBKS have been successfully used to attitude tracking of fixed-wing aircraft [1,11,12,18,19]. The attitude tracking is commonly developed in a classic cascade structure as the one presented in Fig. 1. Using the time-scale separation principle, the control is split into two stages, being the outer one responsible for controlling the aircraft attitude angles, and the inner one for controlling the attitude rate.

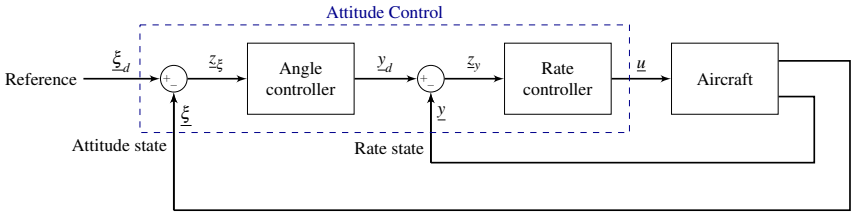

Fig. 1 Cascaded attitude control structure.

Previous works have applied INDI and IBKS as rate controllers, being the outer-loop controller implemented using the traditional nonlinear technique since the attitude kinematics model is considered as known [1, 2, 19]. However, for fixed-wing aircraft looking for a coordinated flight, a common approach is to track the Angle of Sideslip (AoS), which is not a truly kinematics variable of the aircraft and depends on the aerodynamics. To consider the AoS as a kinematics variable, the non-gravitational force components of the AoS dynamics model has to be replaced by measured accelerations.

More recent, [21] proposes the use of a Command-Filtered IBKS applying the incremental approach in both control levels. The technique has multiple command filters to attenuate noises and limit the bandwidth of reference signals.

In this paper, we use a similar solution to the one presented in [21], using the incremental strategy in the outer-loop as well. However, we show that a simpler solution using few differentiators and an Input Scaling Gain [16] is able to solve the attitude tracking problem. Furthermore, we include the airspeed as a tracking variable of the rate controller, resulting in a combined actuation using control surfaces and engine thrust. The advantages of our approach are: 1) the simpler formulation of the control problem; 2) The combined usage of control surfaces and engine thrust to solve the attitude tracking; and 3) the low noise sensitivity in the outer-loop compared to the solution using BKS.

This work results from the ongoing European project INCEPTION[1], which is seeking the development of fault-tolerant AFCS for fixed-wing aircraft allying incremental control strategies, adaptive augmentation and envelope protection. We choose the IBKS strategy in the cascade structure because of its Lyapunov-based stability guarantee, which may facilitate possible certification of the AFCS. To

[1] https://inception-h2020.tekever.com/

validate the results, a simulator of the Boeing 747 is used. The solutions using BKS+IBKS and IBKS+IBKS are compared and their results are evaluated according to the military standard MIL-DTL-9490E for AFCS [22].

The outline of this document is: Section 2 shows considerations about the attitude kinematics model and the rate dynamics model considered for control design; Section 3 develops the proposed cascaded incremental backstepping controller; Section 4 compares the results using the proposed approach (IBKS+IBKS) with the BKS+IBKS solution and evaluates the control performance using military standard; Section 5 presents our final conclusions.

2 Aircraft attitude model

The aircraft can be represented by a nonlinear state-space model:

$$\dot{\underline{x}} = f\left(\underline{x},\, \underline{u}\right) \tag{1}$$

where $\underline{x}$ and $\underline{u}$ are, respectively, the state and input vectors.

To design the controllers we extract the attitude model of the aircraft, separating it in a kinematics model and a rate dynamics model.

2.1 Attitude kinematics model

The considered attitude kinematics model of the aircraft is defined by the roll angle ϕ, the pitch angle θ, and the angle of sideslip β, which are the components of the attitude state vector $\underline{\xi}$. Therefore, the nonlinear state-space model is defined as:

$$\dot{\underline{\xi}} = f_{\xi}\left(\underline{\xi},\, \underline{\omega}\right) \tag{2}$$

where $\underline{\omega}$ is the angular rate vector composed by the roll, pitch and yaw rates (p, q, and r, respectively).

The function f_{ξ} is composed by the kinematics equations of the attitude model. The relation between Euler angles and the angular rates is purely kinematic, while the relation between the AoS and the angular rates is not and depends on the aerodynamics. In fact, the AoS derivative can be expressed as [1]:

$$\dot{\beta} = \tfrac{1}{mV_t}\left[-\left(\bar{X}+F_T\right)\cos\alpha\sin\beta + \bar{Y}\cos\beta - \bar{Z}\sin\alpha\sin\beta + mg_2\right] + p\sin\alpha - r\cos\alpha \tag{3}$$

where m is the aircraft total mass; V_T is the true airspeed; α in the angle of attack; $\bar{X}$, $\bar{Y}$ and $\bar{Z}$ are the components of the aerodynamic forces on the aircraft; and F_T is the thrust force produced by the engines. The term g_2 is the y-axis component of the gravitational acceleration calculated in the wind referential frame, given as [23]:

$$g_2 = g\left(\cos\alpha\sin\beta\sin\theta + \cos\beta\sin\phi\cos\theta - \sin\alpha\sin\beta\cos\phi\cos\theta\right) \tag{4}$$

Note that the force terms $(\bar{X}+F_T)$, $\bar{Y}$ and $\bar{Z}$ are the non-gravitational forces applied on the aircraft. Therefore, we can use the specific forces A_x, A_y and A_z to replace them, which are directly measured by the accelerometers.

Finally, we can represent (2) as the following affine nonlinear model:

$$\dot{\underline{\xi}} = \underline{\mathrm{f}}_{\xi} + \mathbf{T}_{\xi}\underline{\omega} \tag{5}$$

where

$$\underline{\mathrm{f}}_{\xi} = \begin{bmatrix} 0 \\ 0 \\ \frac{1}{V_t}\left(-A_x\cos\alpha\sin\beta + A_y\cos\beta - A_z\sin\alpha\sin\beta + g_2\right) \end{bmatrix} \tag{6}$$

and

$$\mathbf{T}_{\xi} = \begin{bmatrix} 1 & \sin\phi\tan\theta & \cos\phi\tan\theta \\ 0 & \cos\phi & -\sin\phi \\ \sin\alpha & 0 & -\cos\alpha \end{bmatrix} \tag{7}$$

2.2 Rate dynamics model

The rate dynamics model describes the dynamic behavior of the aircraft attitude. The airspeed is added to the rate dynamics model focusing on the design of the aircraft cruise control. Thus, the rate dynamics model can be expressed using a state-space representation as follows:

$$\dot{\underline{y}} = f_y\left(\underline{y}, \underline{u}\right) \tag{8}$$

where the rate state vector $\underline{y}$ is composed by the airspeed V_T and the angular rate vector $\underline{\omega}$. The inputs are the actuators of the aircraft – control surfaces and engines –, which depend on the aircraft structure.

The function f_y corresponds to the dynamics model of the aircraft airspeed and angular rates. In this paper, the rate controller will be developed using ID, not requiring extensive knowledge of the model and, therefore, its mathematical formulation is suppressed here. For details on aircraft dynamics formulation, please refer to [24], or to [25] for a Boeing 747 model.

3 Control design

In this section we formulate the cascaded controllers shown in Fig. 1. The controllers are developed based on incremental dynamics. More precisely, the Incremental Backstepping technique is used for both angle and rate controllers.

3.1 Incremental Dynamics

The ID is a technique to describe system dynamics with partial knowledge of the system model. Let us represent (1) by its Taylor series:

$$\dot{\underline{x}} = \dot{\underline{x}}_0 + \frac{\partial f(\underline{x}_0,\, \underline{u}_0)}{\partial \underline{x}} (\underline{x} - \underline{x}_0) + \frac{\partial f(\underline{x}_0,\, \underline{u}_0)}{\partial \underline{u}} (\underline{u} - \underline{u}_0) + \mathscr{O}(2) \tag{9}$$

where $\underline{x}_0$ and $\underline{u}_0$ are the state and input vectors in a recent previous time t_0, and $\mathscr{O}(2)$ denotes the terms of the Taylor series with order greater than or equal to two.

A system can be described using ID if the following constraints are assumed true:

1. The state and input are bounded and the function $f(\underline{x},\, \underline{u})$ is continuous in all domain;
2. The time interval T_s elapsed between $\underline{x}_0$ and $\underline{x}$ is sufficiently small, such that we can assume $\underline{x}_0 \approx \underline{x}$, considering that state changes are integration of input changes and, therefore, slower.

With these assumptions, the difference $\underline{x} - \underline{x}_0$ and higher order terms are neglected. Thus, (9) reduces to:

$$\dot{\underline{x}} \simeq \dot{\underline{x}}_0 + \underbrace{\frac{\partial f(\underline{x}_0,\, \underline{u}_0)}{\partial \underline{u}}}_{\mathbf{B_0}} (\underline{u} - \underline{u}_0) \tag{10}$$

Equation (10) represents the incremental dynamics of the system, which appears as the derivative increment between the current time and the previous time due to the input increment. If the measurement of $\dot{\underline{x}}_0$ is available, the only needed knowledge of the model is the actuation matrix $\mathbf{B_0}$ estimated at the previous time step t_0.

3.2 Cascaded Incremental Backstepping

The incremental dynamics defined by (10) can be used to obtain controllers inspired in the Backstepping (BKS) approach. In previous work [1, 12, 19], the IBKS is used to obtain the rate controller, while the BKS is used for the angle controller.

Although the attitude kinematics model is indeed known, the computing of (6) requires the precise measurement of accelerations, Euler angles, angle of attack, angle of sideslip and true airspeed.

To increase the control robustness and simplify its implementation, we propose to formulate both angle and rate control using ID. In this solution, we replace the knowledge of $\underline{\mathrm{f}}_{\underline{\xi}}$ in (5) by the measurement of the attitude state derivative ($\dot{\underline{\xi}}$).

3.2.1 Angle controller

Let us consider the attitude kinematics model (2) and the following Candidate Lyapunov Function (CLF):

$$\mathscr{V}_\xi = \frac{1}{2} \underline{z}_\xi^T \underline{z}_\xi \tag{11}$$

where $\underline{z}_\xi = \underline{\xi}_d - \underline{\xi}$ is the kinematics error, with $\underline{\xi}_d$ as the desired kinematics state. Note that $\mathscr{V}_\xi$ is a valid CLF once it is positive for all domain, excluding the origin in which it is equals to zero.

To ensure the asymptotic convergence of the error, the CLF derivative must be strictly negative for $\underline{z}_\xi \neq 0$. Considering a positive definite matrix $\mathbf{W}_\xi$, the CLF is strictly negative if:

$$\dot{\mathscr{V}}_\xi = \underline{z}_\xi{}^T \dot{\underline{z}}_\xi = -\underline{z}_\xi^T \mathbf{W}_\xi \underline{z}_\xi \tag{12}$$

Replace the term $\dot{\underline{z}}_\xi$ of (12) using the incremental dynamics of the kinematics model, and since $\underline{z}_\xi \neq 0$, this condition corresponds to:

$$\dot{\underline{\xi}}_d - \dot{\underline{\xi}}_0 - \mathbf{T}_\xi (\underline{\omega} - \underline{\omega}_0) + \mathbf{W}_\xi \underline{z}_\xi = 0 \tag{13}$$

Let us consider the pseudo-control $\underline{\nu}_\alpha = \underline{\omega}_d$ as the desired angular velocity. The pseudo-control law can be obtained by the inversion of (13) with respect to $\underline{\omega}$, resulting in:

$$\underline{\nu}_\alpha = \underline{\omega}_0 + \mathbf{T}_\xi^{-1} \left(\mathbf{W}_\xi \underline{z}_\xi + \dot{\underline{\xi}}_d - \dot{\underline{\xi}}_0 \right) \tag{14}$$

Fig. 2 shows the block diagram of the IBKS angle controller.

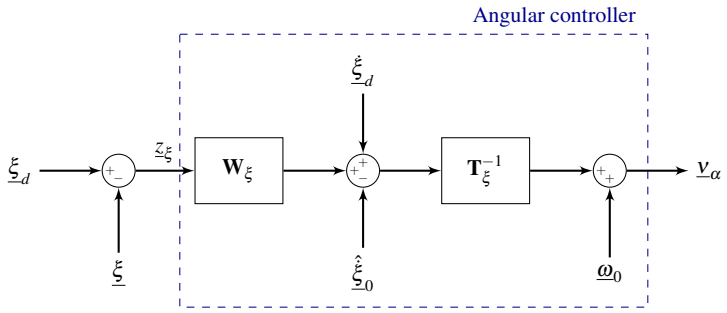

Fig. 2 Block diagram of the IBKS angle controller.

3.2.2 Rate controller

The rate controller is designed as a second IBKS. The desired angular rates are provided by angle controller. The airspeed is introduced as a state in order to design

a rate controller which simultaneously tracks the airspeed and angular rates of the aircraft.

To ensure the asymptotic convergence of the dynamics state $\underline{y} = \left[V_t \ \underline{\omega}^T\right]^T$ towards its desired value $\underline{y}_d = \left[V_{td} \ \underline{\nu}_\alpha^T\right]^T$, let us consider the following CLF:

$$\mathscr{V}_y = \mathscr{V}_\xi + \frac{1}{2a}\underline{z}_y^T \underline{z}_y, \tag{15}$$

where $\underline{z}_y = \underline{y}_d - \underline{y}$, and a is a design scale factor.

The error $\underline{z}_y$ converges asymptotically to zero if the derivative of the CLF $\mathscr{V}_y$ is strictly negative for non-zero errors. Considering a positive definite matrix $\mathbf{W_y}$, the convergence is ensured if:

$$\dot{\mathscr{V}}_y = \dot{\mathscr{V}}_\xi + \frac{1}{a}\underline{z}_y^T \dot{\underline{z}}_y = -\underline{z}_\xi^T \mathbf{W}_\xi \underline{z}_\xi - \frac{1}{a}\underline{z}_y^T \mathbf{W_y} \underline{z}_y \tag{16}$$

Note that $\underline{\omega} = \underline{\nu}_\alpha - \mathbf{C_{y\omega}}\underline{z}_y$, where $\mathbf{C_{y\omega}} = \left[\ \underline{0}_3 \quad \mathbf{I_3}\ \right]$ is a selection matrix such as $\underline{\omega} = \mathbf{C_{y\omega}}\underline{y}$. Thus, we can use (13) and the incremental dynamics representation of $\dot{\underline{y}}$ in (16), leading to:

$$\underline{z}_\xi^T \left(\dot{\underline{\xi}}_d - \dot{\underline{\xi}}_0 - \mathbf{T}_\xi \left(\underline{\nu}_\alpha - \mathbf{C_{y\omega}}\underline{z}_y - \underline{\omega}_0\right) + \mathbf{W}_\xi \underline{z}_\xi\right) + \frac{1}{a}\underline{z}_y^T \left(\dot{\underline{y}}_d - \dot{\underline{y}}_0 - \mathbf{B_y}\left(\underline{u} - \underline{u}_0\right) + \mathbf{W_y}\underline{z}_y\right) = 0 \tag{17}$$

where $\mathbf{B_y}$ is the input matrix with respect to $\underline{y}$, or the matrix obtained from the linearized state-space model of the aircraft.

Finally, for non-zero errors, we can substitute (14) in (17) and solve it with respect to $\underline{u}$, providing the final control law:

$$\underline{u}_c = \underline{u}_0 + \mathbf{B_y^{-1}}\left(a\mathbf{C}_{\mathbf{y}\omega}^T \mathbf{T}_\xi^T \underline{z}_\xi + \mathbf{W_y}(\underline{y}_d - \underline{y}) + \dot{\underline{y}}_d - \dot{\underline{y}}_0\right) \tag{18}$$

In (18), the input matrix $\mathbf{B_y}$ needs to be inverted. If this matrix is not square, a control allocation matrix or pseudo-inverse algorithms can be used.

The main advantage of using incremental techniques is their robustness to unmodeled dynamics since most of it is provided by the measurement of the state derivative. However, sensor-based techniques must be robust to measurement noise. To attenuate the measurement noise and increase the control robustness, it is proposed in [16] to multiply $\mathbf{B_y^{-1}}$ in (18) by a diagonal matrix $\Lambda > 0$ with elements $\lambda_{ii} \in]0,1]$, leading to the following control law:

$$\underline{u}_c = \underline{u}_0 + \mathbf{B_y^{-1}}\Lambda\left(a\mathbf{C}_{\mathbf{y}\omega}^T \mathbf{T}_\xi^T \underline{z}_\xi + \mathbf{W_y}(\underline{y}_d - \underline{y}) + \dot{\underline{y}}_d - \dot{\underline{y}}_0\right) \tag{19}$$

The input scaling gain matrix Λ can be interpreted as an additional low-pass filter, attenuating the noise, but reducing the bandwidth of the closed-loop response as a trade-off.

Fig. 3 shows the block diagram of the IBKS rate controller.

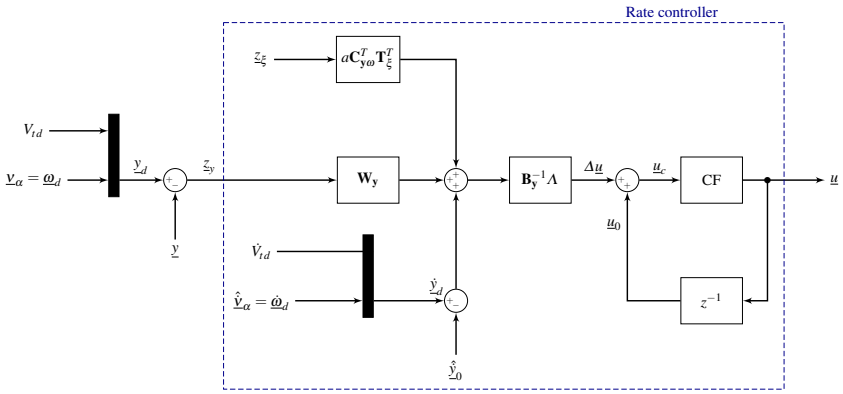

Fig. 3 Block diagram of the IBKS rate controller.

Command filter

To avoid infeasible commands provided by the controller, a Command Filter (CF) is added to the controller output (see Fig. 3). This technique has been used in backstepping strategies, constraining the pseudo-control in each step [6].

For incremental controllers, the CF is used to constrain the input in order to respect the actuators dynamics and saturation. Also, given the integrative characteristics of incremental controllers, it acts as anti-windup. Herein, the CF approximates the actuators as first-order systems with saturation. Fig. 4 presents the proposed CF.

Differentiator

The measurements available may not include all needed variables for the controllers proposed herein, given that state derivatives are often not measured. Also, the control law (19) depends on the derivative of the pseudo-control provided by the angle controller. Therefore, these variables need to be estimated as a function of the measurements.

To estimate signal derivatives, we propose a second-order band-pass filter as a differentiator (see Fig. 5). The differentiator is used to obtain the derivative of the attitude state $\dot{\underline{\xi}}$ (Fig. 2), the rate state $\dot{\underline{y}}$, and the pseudo-control $\dot{\underline{\nu}}_\alpha$ (Fig. 3).

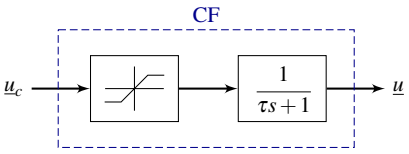

Fig. 4 Proposed command filter.

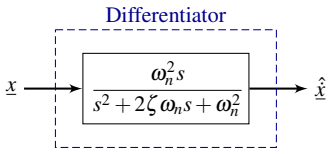

Fig. 5 Proposed state differentiator.

4 Results

The controller using two incremental backstepping stages (IBKS+IBKS) is evaluated for attitude step maneuvers and airspeed step. The step demands are in agreement with the military standard MIL-DTL-9490E [22].

The results of the controlled system are compared with the approach using classical backstepping in the angle controller and IBKS in the rate controller (BKS+IBKS). In this approach, the rate control law is the same of (19), but the pseudo-control $\underline{\nu}_\alpha$ provided by the angular control is different and is given by [1]:

$$\underline{\nu}_\alpha = \mathbf{T}_\xi^{-1}\left(\mathbf{W}_\xi \underline{z}_\xi + \dot{\underline{\xi}}_d - \underline{\mathrm{f}}_\xi\right) \tag{20}$$

Note that (20) is dependent of the angular internal dynamics ($\underline{\mathrm{f}}_\xi$) which has to be calculated for each control iteration.

The controllers are evaluated in a Matlab/Simulink environment using the simulator developed by TU Delft, the B747 GARTEUR RECOVER benchmark simulator [26], with modifications by the Institute of Flight System Dynamics - *Technische Universität München* (FSD-TUM) including custom failure simulation and trim and linearisation.

The Boeing 747 is a large and heavy transportation airplane. It has a length of 70.5 meters, wingspan of 59.6 meters, and the total mass is greater than 250 tons. In a system perspective, as a commercial transportation airplane, the aircraft aims to be safe and, therefore, stable. However, the maneuverability is limited.

The actuation of the Boeing 747 simulator corresponds to four ailerons, four elevators, two rudders, and four engines. Considering the control allocation being solved in the simulator level, we have four generalized actuators as input: aileron (δ_A), elevator (δ_E), rudder (δ_R) and engine thrust (δ_T). With four actuation inputs, $\mathbf{B_y}$ is a square 4x4 nonsingular matrix, which is invertible, not requiring additional allocation.

The nominal condition from which the simulation starts is a straight flight towards North with 340 knot of True Airspeed (TAS) and at an altitude of 5000 ft. The Jacobian matrix corresponding to the derivative of the system by its inputs is obtained numerically in the nominal condition and it is considered constant during the simulation. The control sample rate is 50 Hz.

4.1 Attitude and airspeed tracking

Let us first analyze the response of the controller to independent attitude and airspeed commands. The maneuvers are considered herein as pulse signals starting in time $t = 10\,\mathrm{s}$. The flight is developed under a low turbulence condition defined by a 20-feet wind of $15\,\mathrm{m/s}$ in North direction and a turbulence intensity exceedance probability of 0.01 (see [22] for details).

The following simulations are presented:

1. Roll response: a +5 degree pulse with duration of 40 s (coordinated turn maneuver);
2. Pitch response: a +5 degree pulse with duration of 40 s (climbing maneuver);
3. Sideslip response: a +2 degree pulse with duration of 40 s (skid-to-turn maneuver);
4. Airspeed response: a pulse of +10 percent increase of airspeed with duration of 60 s (straight-and-level acceleration maneuver).

Fig. 6 compares the results obtained using BKS+IBKS and IBKS+IBKS. In the figure, each column presents the aircraft response for one of the maneuvers described above. For example, the first column presents the aircraft response to a roll demand, in which the obtained states ϕ, θ, β, and V_t are shown in rows 1 to 4 respectively.

In Fig. 6, we can see that both solutions have similar responses, with exception for the sideslip angle demand (column 3). During the skid-to-turn maneuver, the errors associated with the computation of $\underline{\mathrm{f}}_{\xi}$ generates an undesired bias error, while for the IBKS+IBKS, no stationary error arises.

Fig. 7 shows the applied control effort during the same simulations. The IBKS+IBKS approach has a noisier actuation than using classical BKS as angular controller, which may be a consequence of controlling the attitude angles based on derivatives.

Regarding the skid-to-turn maneuver – sideslip demand – we can see in Fig. 7 that the rudder reacts faster with the IBKS+IBKS controller. As consequence, the sideslip angle step response with the IBKS+IBKS has a lower settling time (see Fig. 6).

4.2 Disturbance rejection

To evaluate the ability of the controller to reject disturbances, we simulate a straight-and-level flight in a high-turbulence condition along with wind gust.

The simulation starts in the nominal condition: North flight, 340 knot of TAS, and altitude of 5000 ft. The atmosphere condition has a 20-feet wind of $25\,\mathrm{m/s}$ in North-East direction with a turbulence intensity exceedance probability of 10^{-6} (see [22] for details). The gust has an intensity of $50\,\mathrm{km/h}$ with duration of 40 s and starting at $t = 10\,\mathrm{s}$.

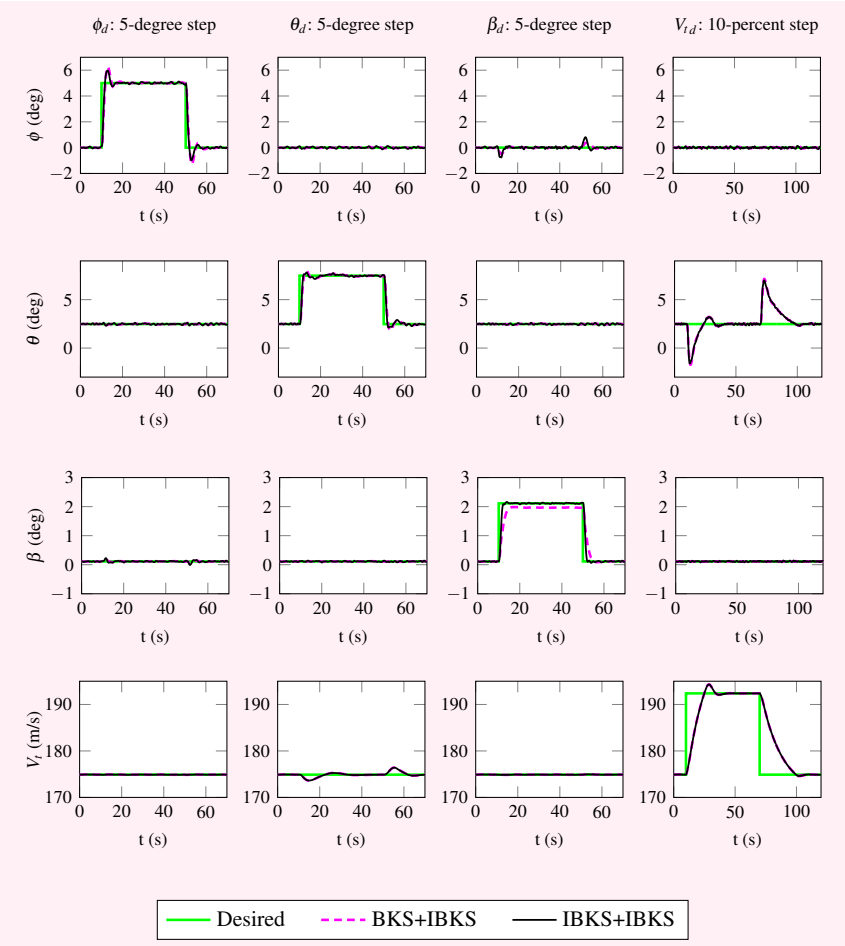

Fig. 6 Simulation responses for demands in roll (column 1), pitch (column 2), sideslip angle (column 3) and airspeed (column 4). The states are ϕ (row 1), θ (row 2), β (row 3), and V_t (row 4).

Fig. 8 and Fig. 9 show the control states and efforts, respectively. Three scenarios were evaluated with gusts in North (only tailwind), East (only crosswind), and North-East (both tailwind and crosswind) direction.

We can see in Fig. 8 that both strategies can reject the disturbances – turbulence and gust – but the IBKS+IBKS has a slightly worse performance rejecting turbulence since its controllers are both based on state derivatives. On the other hand, the sideslip angle during lateral gust is completely regulated by the IBKS+IBKS controller, while a residual AoS can be seen using the BKS+IBKS strategy.

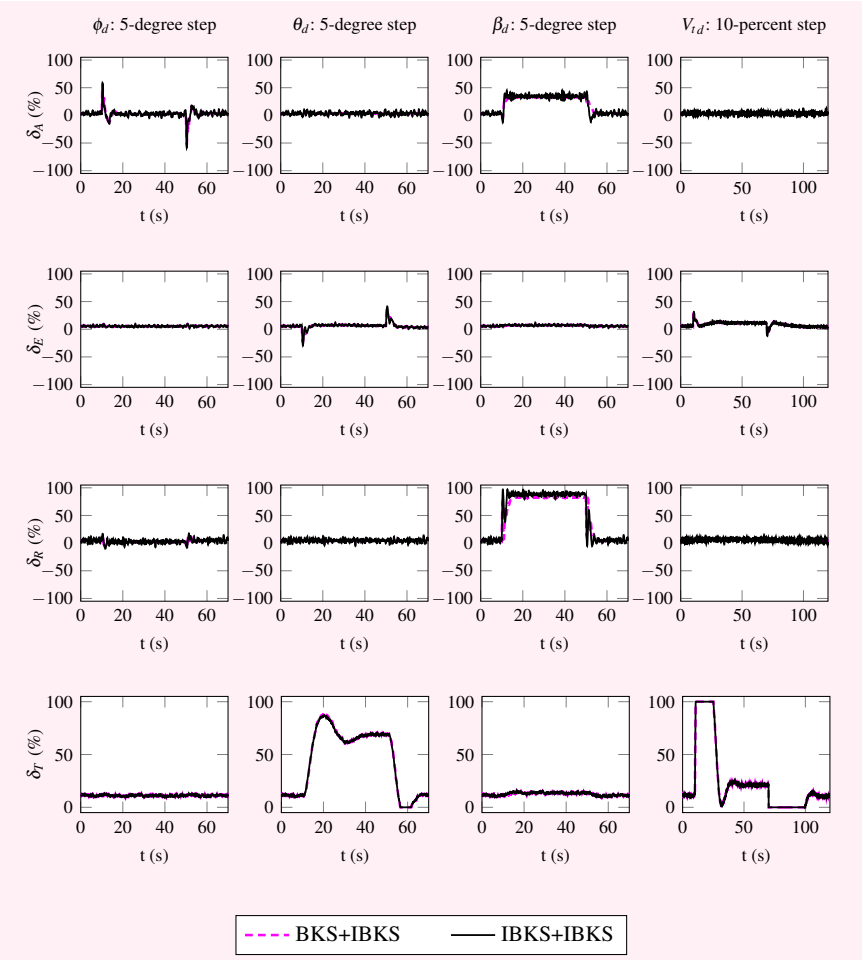

Fig. 7 Control effort for demands of roll (column 1), pitch (column 2), sideslip angle (column 3) and airspeed (column 4). The inputs are δ_A (row 1), δ_E (row 2), δ_R (row 3), and δ_T (row 4).

The control effort (see Fig 9) is very similar in both strategies, being noisier when using the IBKS+IBKS. Note that the rudder is almost saturated in the presence of the east gust.

The simulation results were used to evaluate the controllers performance according to the military standard MIL-DTL-9490E which defines criteria for AFCS [22]. Table 1 summarizes the performance criteria for attitude AFCS and shows that the results obtained with the IBKS+IBKS controller fulfill the requirements.

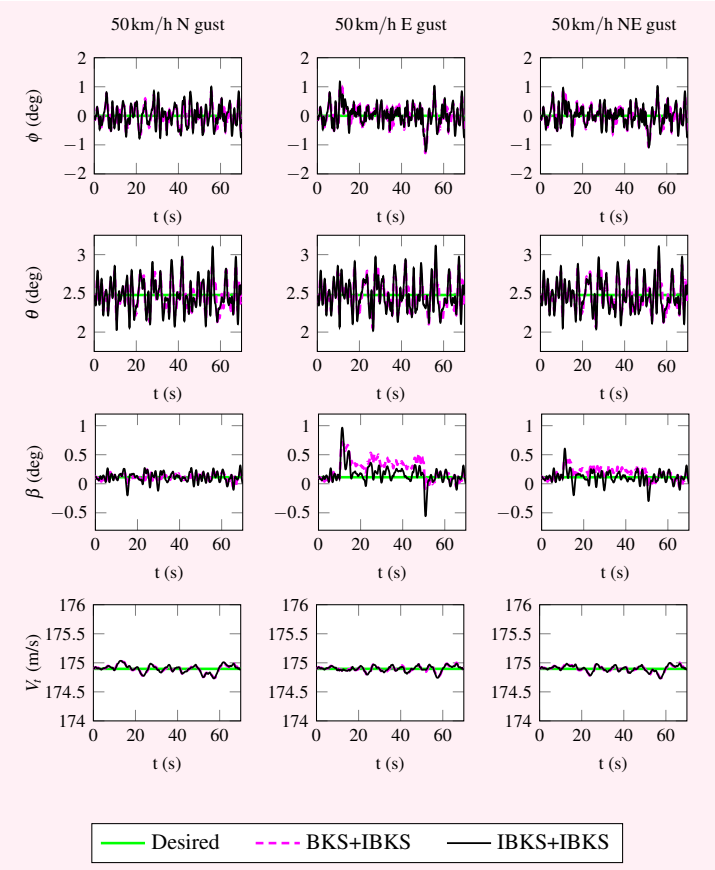

Fig. 8 Disturbance rejection simulation with gust in north (column 1), east (column 2), and north-east (column 3) direction. The states are ϕ (row 1), θ (row 2), β (row 3), and V_t (row 4).

Table 1 Performance evaluation of the IBKS+IBKS controller.

Type	Criteria	Limit	IBKS+IBKS
Roll attitude response	Hold accuracy	0.5^o	0.00^o
	Hold accuracy (turbulence)	5^o RMS	0.03^o RMS
	Settling time (5^o step)	≤ 5 s	3.8 s
Pitch attitude response	Hold accuracy	1^o	0.00^o
	Hold accuracy (turbulence)	10^o RMS	0.01^o RMS
	Settling time (5^o step)	≤ 5 s	1.4 s
Airspeed response	Hold accuracy	6.8 knot	0.02 knot
	Periodicity	≥ 20 s	none
Coordinated turn	Steady-banked lateral acceleration	0.03g	0.006g
	Sideslip angle	2^o	0.11^o
	Maximum lateral acceleration	0.1g	0.082g
Coordinated straight	Lateral acceleration	0.02g	0.005g
	Sideslip angle	2^o	0.11^o

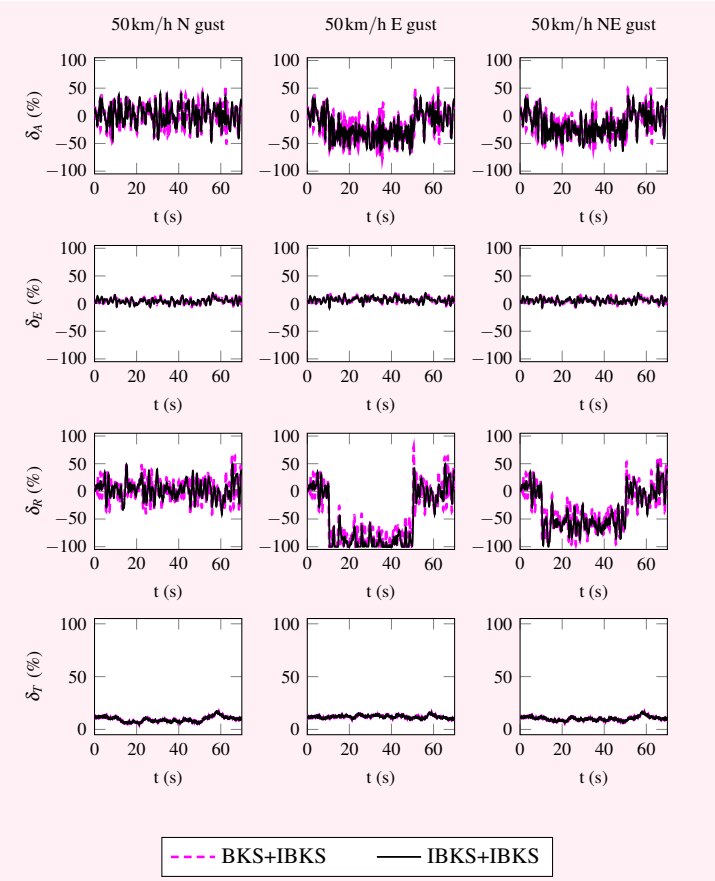

Fig. 9 Control effort to reject turbulence and gust in north (column 1), east (column 2), and north-east (column 3) direction. The inputs are δ_A (row 1), δ_E (row 2), δ_R (row 3), and δ_T (row 4).

5 Conclusion

In this article we formulate an attitude controller using a cascaded approach and applying the incremental backstepping strategy in both levels of the cascaded structure. The proposed strategy is able to correctly track demands in roll, pitch, sideslip angles and airspeed.

Given the robustness of the incremental controller, the estimated state derivative provided by the second-order bandpass filter is accurate enough to control the aircraft attitude angles. Furthermore, using the IBKS instead of the BKS in the angle controller provides a simpler solution, not requiring measurements of accelerations and computation of gravitational acceleration components.

When compared with the BKS+IBKS solution, the performance of the IBKS+IBKS strategy has a clear advantage in tracking AoS. The errors when computing (6) using sensor data produce a stationary error in the tracking of the AoS, which is mitigated using the IBKS solution. Despite skid-to-turn maneuvers are not commonly applied in commercial aviation, it is an important maneuver for small UAVs. The ability to correctly track sideslip angles can also be seen in the rejection of lateral gust.

With the results shown in Table 1, we can conclude that the proposed solution – which is developed using Lyapunov stability theory – has large potential to be used in commercial aviation.

Future work will expand the results presented herein aiming at fault-tolerant controllers. Moreover, the control robustness has to be analyzed when dealing with non-nominal flight conditions, with special attention to changes in the input matrix $\mathbf{B_y}$.

Acknowledgements This research is co-funded by the European Union in the scope of INCEPTION project, which has received funding from the EU Horizon 2020 Research and Innovation Programme under grant agreement No. 723515, and by FCT, through IDMEC, under LAETA, project UID/EMS/50022/2019.

References

1. P. van Gils, E.-J. Van Kampen, C. C. de Visser, and Q. P. Chu, "Adaptive incremental backstepping flight control for a high-performance aircraft with uncertainties," in *AIAA Guidance, Navigation, and Control Conference*, 2016, p. 1380.
2. L. G. Sun, C. C. de Visser, Q. P. Chu, and J. A. Mulder, "Joint sensor based backstepping for fault-tolerant flight control," *Journal of Guidance, Control, and Dynamics*, vol. 38, no. 1, pp. 62–75, 2015.
3. G. J. Balas, "Flight control law design: An industry perspective," *European Journal of Control*, vol. 9, no. 2, pp. 207 – 226, 2003.
4. S. A. Snell, D. F. Enns, and W. L. Garrard Jr., "Nonlinear inversion flight control for a supermaneuverable aircraft," *Journal of Guidance, Control, and Dynamics*, vol. 15, no. 4, pp. 976–984, 1992.
5. S. N. Singh and M. Steinberg, "Adaptive control of feedback linearizable nonlinear systems with application to flight control," *Journal of Guidance, Control, and Dynamics*, vol. 19, no. 4, pp. 871–877, 1996.
6. J. A. Farrell, M. Polycarpou, M. Sharma, and W. Dong, "Command filtered backstepping," *IEEE Transactions on Automatic Control*, vol. 54, no. 6, pp. 1391–1395, June 2009.
7. L. Sonneveldt, "Adaptive backstepping flight control for modern fighter aircraft," Ph.D. dissertation, Technische Universiteit Delft, Netherlands, 2010.
8. K. Bordignon and J. Bessolo, "Control allocation for the x-35b," in *2002 Biennial International Powered Lift Conference and Exhibit*, AIAA. Williamsburg, VA, U.S.A.: American Institute of Aeronautics and Astronautics, 2002.
9. P. Smith, "A simplified approach to nonlinear dynamic inversion based flight control," in *23rd Atmospheric Flight Mechanics Conference*. Boston, MA, U.S.A.: American Institute of Aeronautics and Astronautics, 1998.
10. B. J. Bacon and A. J. Ostroff, "Reconfigurable flight control using nonlinear dynamic inversion with a special accelerometer implementation," in *AIAA Guidance, Navigation, and Control Conference and Exhibit*, Dever, CO, USA, 2000.

11. S. Sieberling, Q. Chu, and J. Mulder, "Robust flight control using incremental nonlinear dynamic inversion and angular acceleration prediction," *Journal of guidance, control, and dynamics*, vol. 33, no. 6, pp. 1732–1742, 2010.
12. P. Acquatella B., "Robust nonlinear spacecraft attitude control: An incremental backstepping approach," Master's thesis, Technische Universiteit Delft, Netherlands, 2011.
13. X. Wang, E.-J. Van Kampen, Q. P. Chu, and P. Lu, "Stability analysis for incremental nonlinear dynamic inversion control," in *2018 AIAA Guidance, Navigation, and Control Conference*, AIAA. Kissimmee, FL, U.S.A.: American Institute of Aeronautics and Astronautics, 2018.
14. H. Chen and S. Zhang, "Robust dynamic inversion flight control law design," in *Systems and Control in Aerospace and Astronautics, 2008. ISSCAA 2008. 2nd International Symposium on*. IEEE, 2008, pp. 1–6.
15. P. Simplício, "Helicopter nonlinear flight control using incremental nonlinear dynamic inversion," Master's thesis, Universidade Técnica de Lisboa, Lisbon, Portugal, 2011.
16. J. Azinheira, A. Moutinho, and J. Carvalho, "Lateral control of airship with uncertain dynamics using incremental nonlinear dynamics inversion," *IFAC-PapersOnLine*, vol. 48, no. 19, pp. 69 – 74, 2015, 11th IFAC Symposium on Robot Control SYROCO 2015.
17. E. Smeur, G. de Croon, and Q. Chu, "Cascaded incremental nonlinear dynamic inversion for mav disturbance rejection," *Control Engineering Practice*, vol. 73, pp. 79 – 90, 2018.
18. F. Grondman, G. Looye, R. O. Kuchar, Q. P. Chu, and E.-J. Van Kampen, "Design and flight testing of incremental nonlinear dynamic inversion-based control laws for a passenger aircraft," in *2018 AIAA Guidance, Navigation, and Control Conference*, AIAA. Kissimmee, FL, U.S.A.: American Institute of Aeronautics and Astronautics, 2018.
19. W. Falkena, "Investigation of practical flight control systems for small aircraft," Ph.D. dissertation, Technische Universiteit Delft, Netherlands, 2012.
20. G. P. Falconí, V. A. Marvakov, and F. Holzapfel, "Fault tolerant control for a hexarotor system using incremental backstepping," in *2016 IEEE Conference on Control Applications (CCA)*, Sept 2016, pp. 237–242.
21. Y. C. Wang, W. S. Chen, S. X. Zhang, J. W. Zhu, and L. J. Cao, "Command-filtered incremental backstepping controller for small unmanned aerial vehicles," *Journal of Guidance, Control, and Dynamics*, vol. 41, no. 4, pp. 954–967, 2018.
22. MIL-DTL-9490E, "Detailed specification: Flight systems - design, installation, and test of piloted aircraft, general specification for," april 2008.
23. L. Sonneveldt, "Nonlinear F-16 model description," Delft University of Technology, The Netherlands, Tech. Rep., June 2006.
24. B. Stevens, F. Lewis, and E. Johnson, *Aircraft Control and Simulation: Dynamics, Controls Design, and Autonomous Systems*, 3rd ed. John Wiley & Sons, Inc., 2016.
25. A. M. Esteban, "A linear parameter varying model of the boeing 747-100/200 longitudinal motion," Master's thesis, University of Minnesota, USA, 2001.
26. H. Smaili, J. Breeman, T. Lombaerts, and D. Joosten, *RECOVER: A Benchmark for Integrated Fault Tolerant Flight Control Evaluation*. Berlin, Heidelberg: Springer Berlin Heidelberg, 2010, pp. 171–221.